Available online at www.sciencedirect.com

ScienceDirect

Journal of Sound and Vibration 311 (2008) 941–952

JOURNAL OF SOUND AND VIBRATION

www.elsevier.com/locate/jsvi

Simulation and experiment of a blind subspace identification method

Zhiyi Zhang*, Jiangling Fan, Hongxing Hua

Institute of Vibration, Shock and Noise, Shanghai Jiao Tong University, Shanghai 200030, PR China

Received 5 July 2007; received in revised form 1 August 2007; accepted 25 September 2007
Available online 26 November 2007

Abstract

A covariance-driven subspace identification method is presented to identify weakly excited modes. In this method, the traditional block Hankel matrix is reshaped to enhance identifiability of weak characteristics. The robustness of eigenparameter estimation to noise contamination is reinforced by the reshaped block Hankel matrix. An alternative stabilization diagram in combination with component energy index (CEI), which indicates vibration intensity of signal components, is adopted to separate spurious and physical modes. Simulation of a vibration system of multiple-degree-of-freedom and experiment of a metallic frame structure subject to wind excitation are presented to demonstrate efficacy of the proposed blind method. The performance of this blind method is assessed in terms of its capability in extracting weak modes as well as the accuracy of estimated parameters. The results have shown that the proposed blind method gives a better estimation of weak modes from response signals of small SNR and gives a reliable separation of spurious and physical estimates.
© 2007 Elsevier Ltd. All rights reserved.

1. Introduction

There are two kinds of modal parameter identification techniques: the conventional with artificial excitation and the blind with natural excitation. Due to the requirement of both input and output measurements, the conventional techniques are inherent with many limitations in practice. In contrast, identification from output only or blind identification has more flexibility [1–4]. In terms of identification domain, blind techniques can be categorized into three groups, i.e. those in the time domain, the frequency domain and the time–frequency domain. In the time domain, subspace methods, which are constructed on the controllability and observability properties of linear time-invariant (LTI) systems, have such attributes as robust and efficient numerical computation and excellent accuracy of estimation. Since 1990s, subspace techniques have been applied successfully to the area of modal parameter identification [5–8].

Generally, the motion of a vibrating structure can be described by the state-space model. In terms of data used in the construction of algorithms, there are two distinguished subspace identification methods: the covariance-driven method and the data-driven method [3,9]. It has been observed that similar mathematical

*Corresponding author.
E-mail address: chychang@sjtu.edu.cn (Z. Zhang).

0022-460X/$ - see front matter © 2007 Elsevier Ltd. All rights reserved.
doi:10.1016/j.jsv.2007.09.051

representations exist between the output covariances and impulse responses of a LTI system excited by white-noise loads [10]. This property reveals that the covariance-driven subspace method is to some extent equal to the eigensystem realization algorithm (ERA) [10–12]. Recently, many research efforts have been made to subspace methods for the improvement of identification of system matrices of the state-space model, and the two algorithms were compared in various ways [11,13,14]. Subspace techniques need linear algebra operations, such as singular value decomposition (SVD) or QR factorization to eliminate noise as well as reduce computation complexity. In addition to SVD, many other operations can be utilized to reject noises in the covariance-driven subspace method where noise elimination and parameter identification are realized separately and accurate estimation can be obtained. Compared to the covariance-driven subspace method, the data-driven method uses projection of the row space of future outputs into the row space of past outputs without any computation of covariances. Therefore, noise rejection is united with parameter identification, but this process results in a heavy computation load.

Due to insufficient environmental excitation or improper locations of measurement points, some modes will carry relatively weak information in a real testing. Traditional subspace methods have some difficulties in the identification of weak modes. Based on the covariance-driven subspace method, the block Hankel matrix is reshaped and accordingly the signal subspace is changed, which leads to an increased participation of weak components and the identifiability of weak characteristics. Noise filtering has a strong impact on the accuracy of estimates. Sometimes weak modal signals may be filtered as noises. Therefore, it is necessary to use a model of redundant order to model weak modes. As a result, spurious modes are generated. SVD and QR factorization are usually utilized to determine the order of the state-space model and to filter noises [15–18]. Spurious modes are the outcome of numerical approximation, and their occurrence depends on model order and the size of data used in approximation. For blind subspace identification, it is even more difficult to get rid of spurious modes. SVD and QR factorization are not always reliable in order determination and must be reinforced.

In this paper, component energy index (CEI) used to measure vibration intensity of signal components [4] is combined with an alternative stabilization diagram to identify spurious and physical modes, which enhances the noise filtering capability of subspace identification methods and results in a better estimation of the weak modal characteristics from response signals of small SNR.

2. The covariance-driven subspace identification method

2.1. Construction of block Hankel matrix

The dynamic behavior of a LTI system can be described by the discrete state-space model [5,14]:

$$\begin{aligned} x(k+1) &= Ax(k) + Bw(k), \\ y(k) &= Cx(k) + Dw(k), \end{aligned} \tag{1}$$

where $x(k) \in R^N$ is the state vector, $y(k) = (y_1, y_2, \ldots, y_L)^{\mathrm{T}} \in R^L$ is the measured output, $w(k) \in R^P$ is assumed to be zero-mean Gaussian white noise with covariance matrix $E(w(k)w(k)^{\mathrm{T}}) = I(I \in R^{P \times P}$ is the identity matrix), k is the discrete time and $k \geqslant 0$. $A \in R^{N \times N}$, $B \in R^{N \times P}$, $C \in R^{L \times N}$ and $D \in R^{L \times P}$ are, respectively, the system matrix, the input matrix, the output matrix and the direct transmission matrix. P and L are the numbers of input and output, respectively. N is the model order.

The recursive structure of the above discrete state model implies the following equation:

$$\begin{aligned} \theta(i+1) &= A\theta(i) + B\sigma(i), \\ r(i) &= C\theta(i) + D\sigma(i), \end{aligned} \tag{2}$$

where $r(i)$, under the ergodicity assumption, is given by

$$r(i) = E(y(k)y^{\mathrm{T}}(k-i)) = \lim_{M \to \infty} \frac{1}{M} \sum_{k=i}^{M+i-1} y(k)y^{\mathrm{T}}(k-i), \quad M > 0, \quad i = 0, 1, 2, \ldots \tag{3}$$

and $\theta(i)=E(x(k)y^{\mathrm{T}}(k-i))$, $\sigma(i)=E(w(k)y^{\mathrm{T}}(k-i))$, $i=0,1,2,\ldots$. Since the available data are limited in quantity, the autocorrelation and cross-correlation can only be estimated with limited data. According to the definition of cross-correlation, there holds $\sigma(i)=0, \forall i \geqslant 1$. Therefore, from Eq. (2), one can obtain

$$R=\Gamma\Theta, \tag{4}$$

where R, Γ and Θ are, respectively, the block Hankel matrix, the extended observability matrix and the extended controllability matrix

$$R=\begin{bmatrix} r(1) & r(2) & \cdots & r(q) \\ r(2) & r(3) & \cdots & r(q+1) \\ \vdots & \vdots & \ddots & \vdots \\ r(p) & r(p+1) & \cdots & r(p+q-1) \end{bmatrix}_{pL\times qL}, \quad \Gamma=\begin{bmatrix} C \\ CA \\ \vdots \\ CA^{p-1} \end{bmatrix}, \quad \Theta=(\theta(1),\theta(2),\ldots,\theta(q)), \quad pL, qL>N.$$

As defined in Eq. (2), $r(i)\in R^{L\times L}$ is a square matrix, i.e.

$$r(i)=\begin{bmatrix} r_{11}(i) & r_{12}(i) & \cdots & r_{1L}(i) \\ r_{21}(i) & r_{22}(i) & \cdots & r_{2L}(i) \\ \vdots & \vdots & \ddots & \vdots \\ r_{L1}(i) & r_{L2}(i) & \cdots & r_{LL}(i) \end{bmatrix}_{L\times L},$$

which contains auto-correlation of each output signal at instant i. Since cross-correlation may result in an insufficient contribution of weak signal components to the block Hankel matrix R, the elements of R are necessary to be regrouped to enhance the identifiability of weak modes. Here, we reconstruct the block Hankel matrix with the diagonal elements of $r(i)$. In terms of these diagonal elements, we define

$$\bar{r}(i)=\mathrm{vec}(\mathrm{diag}(r(i))), \quad i=0,1,2,\ldots, \tag{5}$$

i.e. $\bar{r}(i)=(r_{11}(i),r_{22}(i),\ldots,r_{LL}(i))^{\mathrm{T}}$. Let $\bar{r}_m(i)=r_{mm}(i)=E(y_m(k)y_m^{\mathrm{T}}(k-i))$ be divided by the maximal absolute value of the M samples, i.e. $\hat{r}_m(i)=\bar{r}_m(i)/\max_{i=1}^{M}(|\bar{r}_m(i)|)$, $\hat{r}(i)=(\hat{r}_1(i),\hat{r}_2(i),\ldots,\hat{r}_L(i))^{\mathrm{T}}$, the reshaped Hankel matrix $\hat{R}$ is thereby constructed as follows:

$$\hat{R}=\begin{bmatrix} \hat{r}(1) & \hat{r}(2) & \cdots & \hat{r}(q) \\ \hat{r}(2) & \hat{r}(3) & \cdots & \hat{r}(q+1) \\ \vdots & \vdots & \ddots & \vdots \\ \hat{r}(p) & \hat{r}(p+1) & \cdots & \hat{r}(p+q-1) \end{bmatrix}_{pL\times q}. \tag{6}$$

Accordingly, this matrix contains normalized auto-correlations of the measured signals, from which natural frequencies and damping ratios can also be estimated.

2.2. Estimation of frequencies and damping ratios

As a special case of the factorization in Eq. (4), the following factorization exists for the signal of the mth channel ($m=1\sim L$):

$$\hat{R}_m=\begin{bmatrix} \hat{r}_m(1) & \hat{r}_m(2) & \cdots & \hat{r}_m(q) \\ \hat{r}_m(2) & \hat{r}_m(3) & \cdots & \hat{r}_m(q+1) \\ \vdots & \vdots & \ddots & \vdots \\ \hat{r}_m(p) & \hat{r}_m(p+1) & \cdots & \hat{r}_m(p+q-1) \end{bmatrix}_{p\times q} = \begin{bmatrix} C_m \\ C_mA \\ \vdots \\ C_mA^{p-1} \end{bmatrix}[\theta_m(1),\theta_m(2),\ldots,\theta_m(q)]=\Gamma_m\Theta_m, \tag{7}$$

where C_m is the measurement vector, $\theta_m(i)=E(x(k)y_m^{\mathrm{T}}(k-i))$, $i\geqslant 1$. Therefore, the range space of $\hat{R}_m$ is equivalent to that of the matrix Γ_m. In consideration of Eq. (7), $\hat{r}(i)=(\hat{r}_1(i),\hat{r}_2(i),\ldots,\hat{r}_L(i))^{\mathrm{T}}$ can be taken as the impulse responses of a system that has the same poles as system (2), thereby Eq. (8) can be deduced:

$$\mathrm{range}(\hat{R}) = \mathrm{range}(\hat{\Gamma}), \tag{8}$$

where

$$\hat{\Gamma} = \begin{bmatrix} \tilde{C} \\ \tilde{C}\tilde{A} \\ \vdots \\ \tilde{C}\tilde{A}^{p-1} \end{bmatrix}, \quad \tilde{A} = \begin{bmatrix} A & & 0 \\ & \ddots & \\ 0 & & A \end{bmatrix}, \quad \tilde{C} = \begin{bmatrix} C_1 & & 0 \\ & \ddots & \\ 0 & & C_L \end{bmatrix}.$$

Since $\hat{r}(i)$ is estimated from a finite number of samples, noises are inevitably present in $\hat{R}$. In order to filter noises, SVD is usually used to separate the signal and noise subspaces:

$$\hat{R} = [U_1 U_2]\begin{bmatrix} \Sigma_1 & \\ & \Sigma_2 \end{bmatrix}\begin{bmatrix} V_1^{\mathrm{T}} \\ V_2^{\mathrm{T}} \end{bmatrix} = U_1\Sigma_1 V_1^{\mathrm{T}} + U_2\Sigma_2 V_2^{\mathrm{T}}, \tag{9}$$

where Σ_1 and Σ_2 are diagonal matrices and Σ_1 has the N dominant singular values. Accordingly, the first item $U_1\Sigma_1 V_1^{\mathrm{T}}$ in Eq. (9) is less contaminated than $U_2\Sigma_2 V_2^{\mathrm{T}}$ and usually regarded as a filtered estimate of $\hat{R}$

$$U_1 = \begin{bmatrix} u_1(1) & u_1(2) & \cdots & u_1(N) \\ u_1(2) & u_1(3) & \cdots & u_1(N+1) \\ \vdots & \vdots & \ddots & \vdots \\ u_1(p) & u_1(p+1) & \cdots & u_1(p+N-1) \end{bmatrix}_{pL\times N}, \quad N<q. \tag{10}$$

According to the shift structure of $\hat{\Gamma}$, matrix A can be estimated as

$$A = U_1^{+}(1:\alpha L, 1:N)U_1(L+1:(\alpha+1)L, 1:N), \tag{11}$$

where $U_1(1{:}L,1{:}N)$ is a submatrix formed by the first L rows and the first N columns of U_1, U_1^{+} is the generalized inverse of U_1, α satisfies $\alpha L>N$. Natural frequencies and damping ratios are then computed as

$$\begin{aligned} f_j &= \left|f_s \ln(\lambda_j)\right|/2\pi, \\ \xi_j &= -\,\mathrm{Re}(f_s \ln(\lambda_j))/\left|f_s \ln(\lambda_j)\right|, \quad j = 1\sim N, \end{aligned} \tag{12}$$

where $\{\lambda_j\}$ are eigenvalues of A, f_s is the sampling frequency.

2.3. Order determination of the model

Theoretically, there should exist a great gap between the two singular value matrices Σ_1 and Σ_2. When there is a significant gap between two consecutive singular values, the state-space model order can be determined easily [16,17]. In practical identification, however, no apparent gap may be observed due to noise corruption. Moreover, order determination on dominant singular values will yield an underestimated model, which will result in estimates of low precision and even missing of weak physical modes. In order to retain all physical modes, especially those of small energy, model order or the column number of $\hat{U}_1$ should be chosen sufficiently large, which leads to a redundant model. According to our experiences, the following principles are adopted to estimate the order:

(1) If a great change occurs in the slope of $\log_{10}(s_{i+1}/s_i)$, an even order $n_1 = (1.5\text{–}2)i$ may be selected, where s_{i+1} and s_i are two consecutive singular values of the block Hankel matrix $\hat{R}$.
(2) If $20\log_{10}(s_1/s_i) = 20\text{–}40\,\mathrm{dB}$, an even order $n_2 \approx i$ may be selected, where s_1 and s_i are the first and the ith singular value of the block Hankel matrix $\hat{R}$, respectively.
(3) The preferable number is $n = \max(n_1,n_2)$.

2.4. Component energy index (CEI)

Due to the redundancy of model order, spurious characteristics always exist in the estimates of Eq. (12). As mentioned earlier, singular values usually fail to indicate an exact model order, and thus cannot be used to discriminate spurious and physical modes without other criteria. Here, we apply the CEI to indicate energy contribution of each signal component [4]. According to CEI, energy information of spurious and physical modes is exhibited, from which we can primitively judge which estimate is reliable.

2.5. Stabilization diagram

Stabilization diagram is usually used to show the variation of estimated modal parameters. The stability or recurrence of estimates can reveal to some extent the existence of physical modes and reliability of estimation. Since model order is redundant, spurious modes will also occur in the diagram. With the increase of model order or fitting data, variation of estimates can be shown explicitly. In constructing a stabilization diagram, the number of fitting data or model order can be set as a variable. When using a variable set of fitting data, an alternative diagram is obtained, which is different from the commonly used one. In this case, the number of rows of $\hat{R}$ will increase while the number of columns is fixed.

Stabilization diagram can be regarded as a measure to evaluate whether one identification method is better than another. For a method of good performance, the stable poles corresponding to physical modes can be clearly indicated in the stabilization diagram and spurious poles are sparsely and randomly distributed. Moreover, for a common method, only as the model order or the row number of Hankel matrix is large enough, can weak modes come to be stable. But for a good identification method, the dimensions of Hankel matrix can be reduced.

The procedure for generating a stabilization diagram is given as follows:

(1) Determine the model order n according to the empirical principles as described above.
(2) Construct a submatrix $U_1(1{:}\beta L{,}1{:}n)$, β is an integer.
(3) Estimate A from $U_1(1{:}\beta L{,}1{:}n)$ according to Eq. (11), i.e. $A = U_1^{+}(1:\alpha L, 1:N)U_1(L+1:(\alpha+1)L, 1:N)$.
(4) Compute frequencies, damping ratios according to Eq. (12).
(5) Normalize CEI, i.e. $\mathrm{CEI}(j) = \mathrm{CEI}(j)/\max_{j=1}^{n}(\mathrm{CEI}(j))$. Those modes corresponding to the normalized CEI less than a prescribed value, for instance, 0.2, may be discarded as spurious modes.
(6) Increase $\beta(\beta+1 \to \beta)$ and go to step (2).

2.6. Estimation of mode shapes

As given previously, frequencies and damping ratios can be estimated by Eqs. (11) and (12). However, mode shapes cannot be extracted from the reshaped block Hankel matrix $\hat{R}$ since it has lost phase information of signal components. Therefore, cross-correlation or the block Hankel matrix R should be used to extract mode shapes, as given in the following procedure:

(1) Choose a reference signal, which has a relatively high SNR, for example, the lth response signal, $1 \leqslant l \leqslant L$.
(2) Construct a submatrix of q columns from the block Hankel matrix R, i.e. $R(1{:}L{,}l{:}L{:}(q-1)L+l)$.
(3) Perform SVD of R, i.e. $R = U_s\Sigma_s V_s^{\mathrm{T}} + U_n\Sigma_n V_n^{\mathrm{T}}$, where s and n stand for signal and noise, respectively.
(4) Construct the Vandermonde matrix $E[\Lambda_1,\Lambda_2,\ldots,\Lambda_N]$, where $\Lambda_j = (1 \quad \lambda_j \quad \cdots \quad \lambda_j^{q-2} \quad \lambda_j^{q-1})^{\mathrm{T}}, j = 1{\sim}N$.
(5) Compute mode shapes

$$\psi = E^{+}R_s^{\mathrm{T}}(1:L, l:L:(q-1)L+l), \quad R_s = U_s\Sigma_s V_s^{\mathrm{T}}. \tag{13}$$

(6) Normalize the mode shapes:

$$\phi(j,:) = \psi(j,:)/\psi(j,l), \quad \phi(j,:) \leftarrow \phi(j,:)/\|\phi(j,:)\|, \quad j = 1{\sim}N. \tag{14}$$

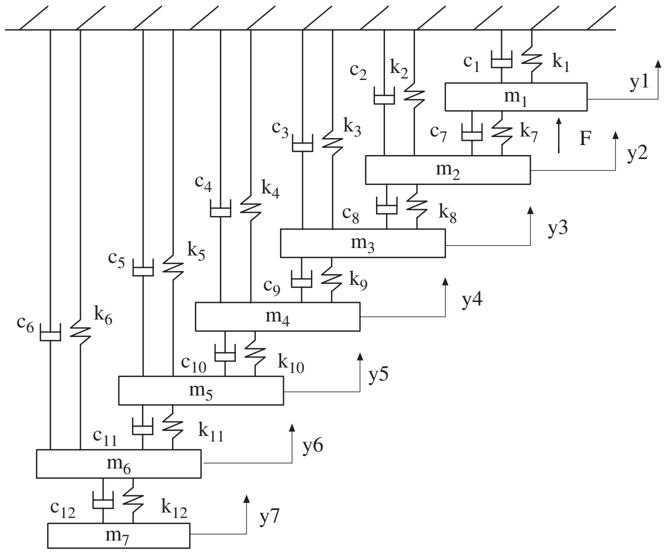

Fig. 1. The vibration system of seven degrees of freedom.

Table 1
Physical parameters of the system

i	1	2	3	4	5	6	7	8	9	10	11	12
m_i (kg)	0.2	0.3	0.5	0.6	0.8	1.1	1.5	–	–	–	–	–
c_i (N s m^{-1})	10	10	10	10	10	10	5	5	5	5	5	5
k_i (kN m^{-1})	500	350	200	80	40	3	450	320	150	50	15	2

Table 2
Frequencies and damping ratios of the system

i	1	2	3	4	5	6	7
f_i	5.445	20.027	53.971	98.09	164.86	259.34	396.31
ξ_I	3.910	6.881	3.432	2.483	1.874	1.721	1.863

3. Simulation

3.1. Model description

The proposed subspace method is applied to a seven-dof system that is excited by an unmeasured force F at the mass m_1, as shown in Fig. 1. Physical parameters of this system are given in Table 1. Natural frequencies and damping ratios are listed in Table 2, where i represents mode order, f_i (Hz) and ξ_i (%) are the ith theoretical frequency and damping ratio, respectively. White-noise excitation is exerted. Acceleration responses are measured at each mass simultaneously at the sampling rate of 1000 Hz and 8000 samples are recorded at each channel. SNR of each response signal is 10 dB.

3.2. Parameter estimation

The proposed subspace method is first compared with FDD. For FDD, noise filtering is also realized by SVD. Singular values are plotted in Fig. 2, which reveals that there exists a great discrepancy in component

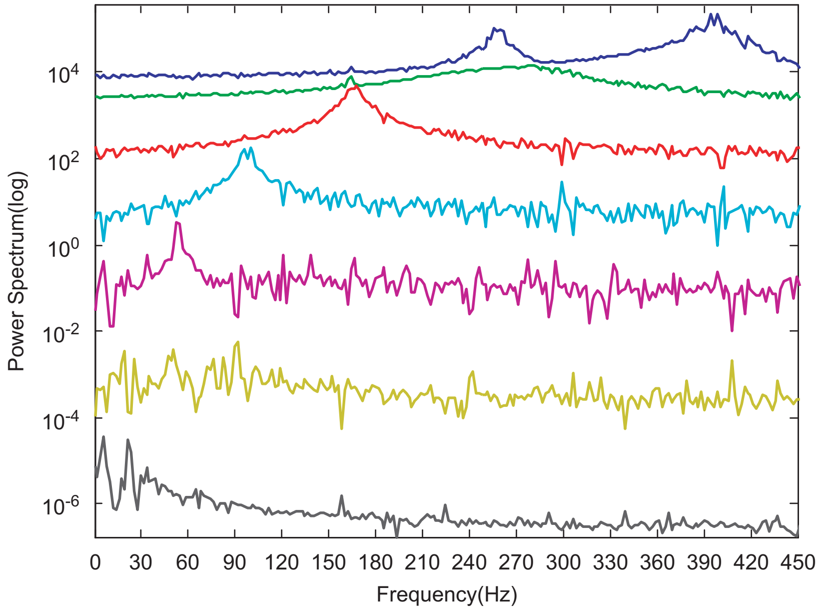

Fig. 2. SVD of power spectrums.

Table 3
Estimated results-FDD [19]

i	1	2	3	4	5	6	7
$\hat{f}_i$	–	21.383	60.537	99.627	168.74	294.14	393.71
e_{fi} (%)	–	6.77	12.168	1.567	2.329	13.436	0.654
$\hat{\xi}_i$	–	9.941	4.173	2.251	2.126	1.126	0.963
$e_{\xi i}$ (%)	–	44.5	21.591	9.343	13.447	34.573	48.309

Table 4
Estimated results-the traditional method

i	1	2	3	4	5	6	7
$\hat{f}_i$	–	–	–	99.235	164.47	264.23	393.06
e_{fi}	–	–	–	1.167	0.236	1.886	0.820
$\hat{\xi}_i$	–	–	–	2.843	2.937	3.639	2.911
$e_{\xi i}$	–	–	–	14.494	56.742	111.44	56.265

energy. This is the reason why $\bar{r}(i)$ is normalized before the construction of Hankel matrix. The estimated results by FDD are given in Table 3, where $\hat{f}_i$ (Hz) and $\hat{\xi}_i$ (%) are the ith estimated frequency and damping ratio, e_{fi} (%) and $e_{\xi i}$ (%) are the relative errors between the estimated and exact frequencies and damping ratios, respectively.

From Table 3 we can see that the estimation error of the first mode is much higher than others and parameters of the second mode are not yet available, which is attributed to the low SNR and small energy of the first two modes. The weak characteristics of the first two modes are in fact blurred by noises.

For the purpose of comparison, estimation is redone by the traditional and proposed subspace methods. According to the principles given in Section 2, model order is chosen to be 30. Using the Hankel matrices R and $\hat{R}$, respectively, frequencies and damping ratios are estimated, as shown in Tables 4 and 5. According to

Table 5
Estimated results-the proposed method

i	1	2	3	4	5	6	7
$\hat{f}_i$	5.592	19.846	53.734	97.591	164.48	259.51	395.47
e_{fi} (%)	2.699	0.905	0.439	0.508	0.229	0.064	0.211
$\hat{\xi}_i$	5.722	9.017	2.923	3.554	1.471	1.448	1.475
$e_{\xi i}$ (%)	46.332	31.046	14.831	43.132	21.516	15.869	20.821

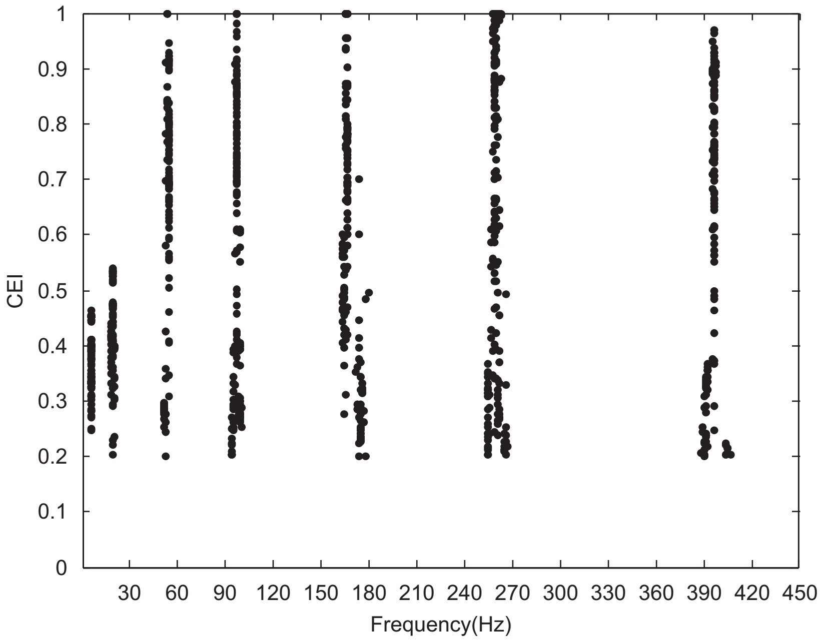

Fig. 3. Normalized CEIs of estimated modes.

these results, performance of the proposed method is clearly demonstrated. Moreover, a clear indication of physical modes is given by the normalized CEIs in Fig. 3, where those modes, corresponding to CEIs less than 0.2, are discarded. Fig. 4 is the stabilization diagrams derived by the two subspace methods, respectively, where data increments are related to row increments of the block Hankel matrices R and $\hat{R}$.

4. Identification of a metallic frame structure subject to wind load

4.1. Configuration and data acquisition

The proposed subspace identification method is used to estimate modal parameters from the acceleration responses of a frame structure excited by wind load. Fig. 5 shows a schematic representation of the metallic frame as well as the placement of accelerometers (p1–p12). As illustrated in the figure, the frame is suspended by a rubber band attached to its center. The suspension frequency is less than 3 Hz, far lower than the first mode of the frame. Wind excitation is simulated by a blower, which is placed more than 5 m away from the frame in order to guarantee the randomicity of excitation. Since the rotating speed of the blower is stable, the frame responses can be regarded as stable random processes. Acceleration responses are recorded simultaneously in two orthogonal directions (y and z) with a sampling rate of 325.52 Hz and the recording time is approximately 50 s. Fig. 6 is the acceleration response of p1.

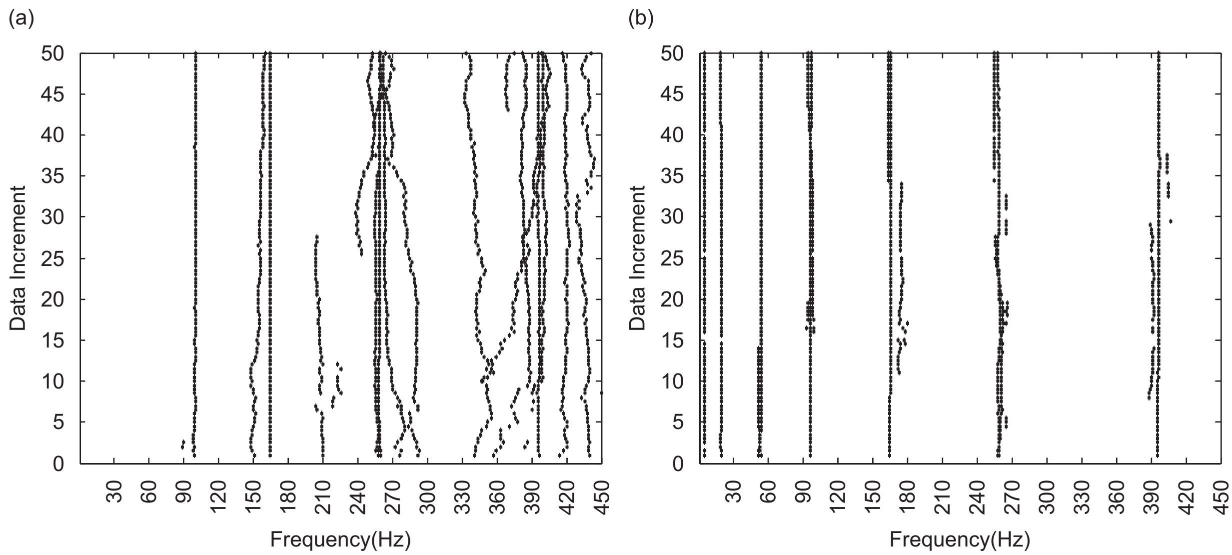

Fig. 4. Stabilization diagram obtained by (a) $R(1{:}\beta L{,}1{:}n)$ and (b) $\hat{R}(1:\beta L,1:n)$.

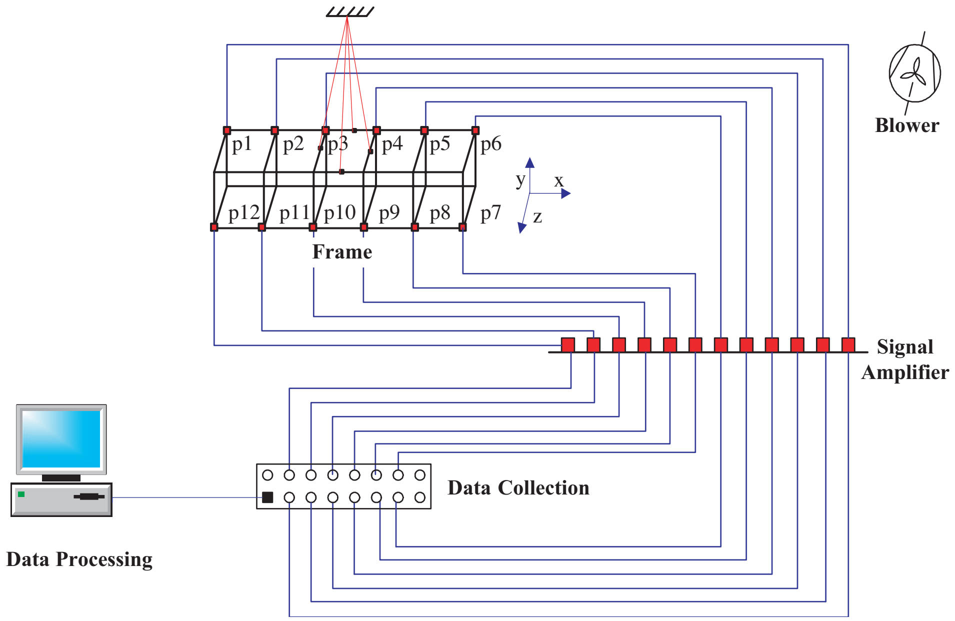

Fig. 5. Test configuration and measurement positions.

4.2. Modal parameter identification

Natural frequencies and mode shapes of the frame structure can be accurately computed by FEM. For the purpose of comparison, computed frequencies are given along with the estimated results in Table 6, where only the first four modes are listed. Before the estimation of system matrix, model order is set to 36 according to the empirical principles. The stabilization diagram and the normalized CEIs in Fig. 7 indicate that there exist four modes in the lower frequency range. Especially, the estimated frequencies keeps almost unchanged to the row increments of $\hat{R}$. This demonstrates the proposed identification method is insensitive to weak response signals.

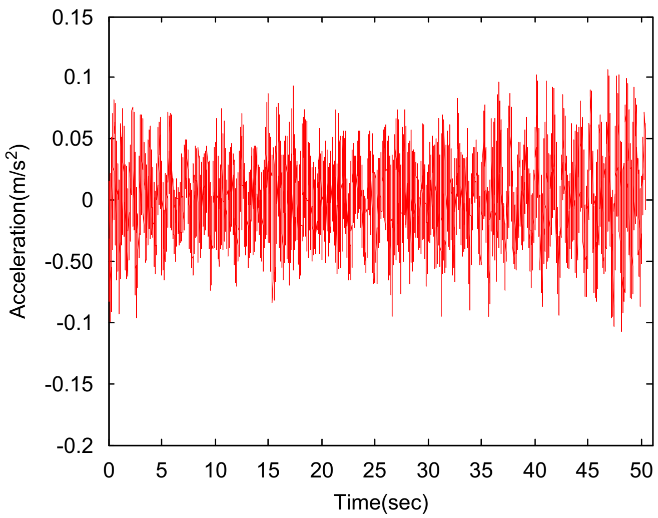

Fig. 6. Acceleration response of p1.

Table 6
Natural frequencies by FEM and the proposed subspace method

I	1	2	3	4
f_i (FEM)	23.423	38.052	48.112	53.783
$\hat{f}_i$	22.941	38.345	47.26	52.841
e_{fi}	2.059	0.771	1.771	1.751

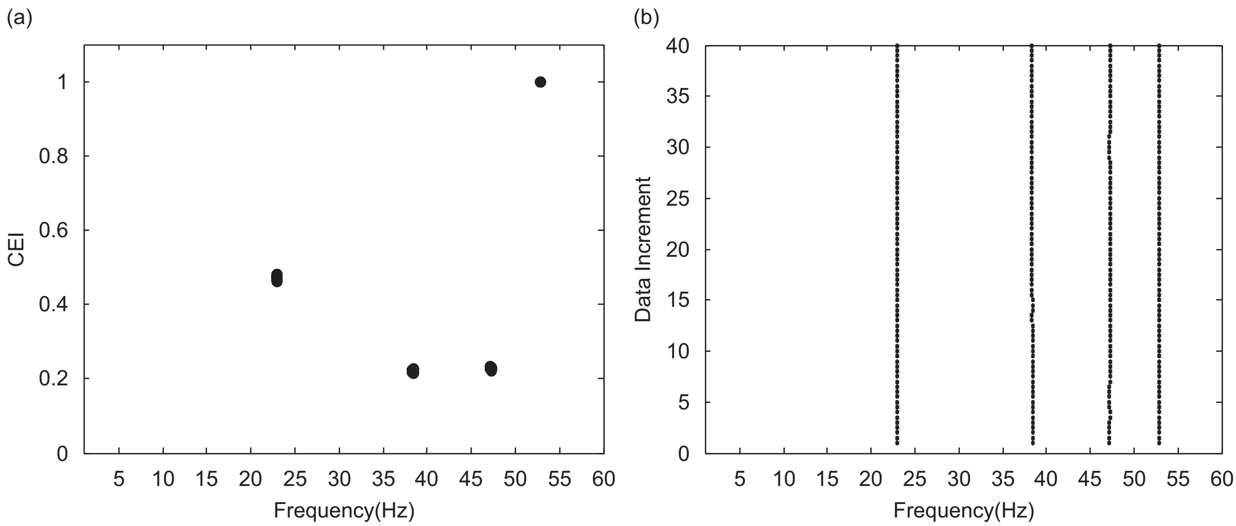

Fig. 7. (a) Distribution of normalized CEIs and (b) stabilization diagram.

Once frequencies and damping ratios are obtained, mode shapes can be estimated according to the procedure given in Section 2.5. Response of p1 is chosen as the reference signal since this point is away from any node of the four mode shapes and accordingly the reference has the highest SNR. Fig. 8 gives the first four normalized mode shapes. For the sake of clarity, only six points (p1–p6) are involved in the illustration of mode shapes. The first and the fourth modes are torsional modes with anti-symmetric ends. The second and

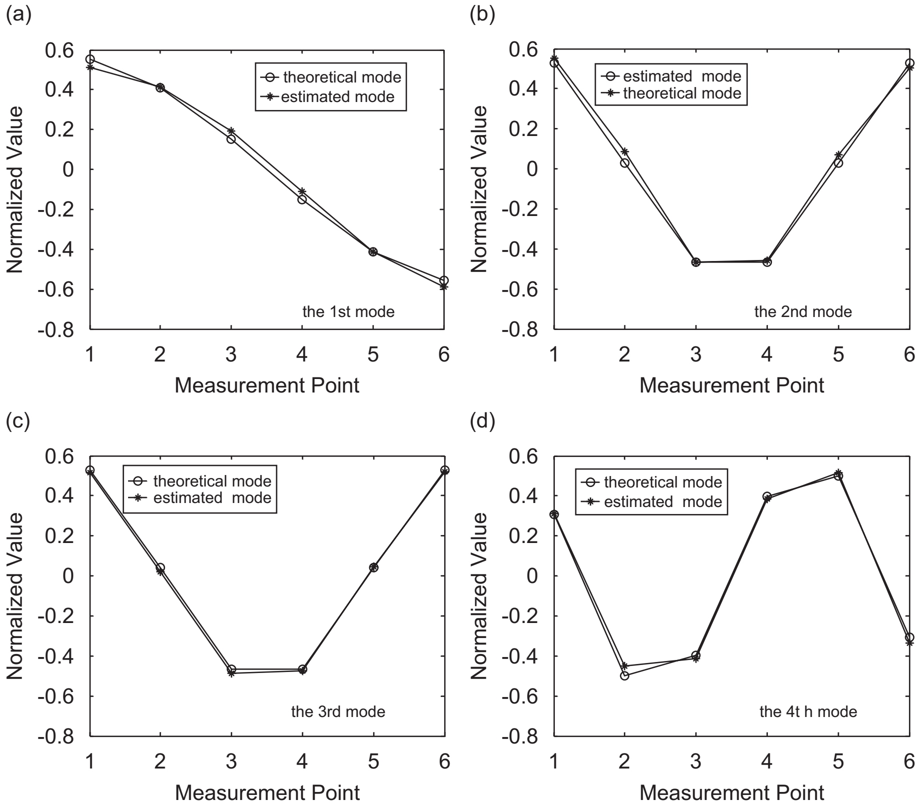

Fig. 8. Comparison of the theoretical and estimated mode shapes: (a) the first mode shape, (b) the second mode shape, (c) the third mode shape and (d) the fourth mode shape.

the third modes are bending modes. As illustrated, mode shapes given by FEM are almost the same as those by identification.

5. Conclusions

In the identification of modal parameters of systems subject to ambient excitation, low identifiability of weak characteristics often renders the problem very challenging. The conventional covariance-driven subspace method is difficult to some extent to identify weak characteristics as compared to the proposed method. The reshaped block Hankel matrix increases the identifiability of weak components and thereby enhances the robustness of estimation to noise contamination. In combination with CEI, the alternative stabilization diagram, which shows the variation or stabilization of modal parameters with the row increments of the block Hankel matrix $\hat{R}$, can effectively indicate spurious modes. Simulation and experiment results have demonstrated good performance of the proposed subspace method, especially for those measurements with low SNR or great energy discrepancy in signal components.

Acknowledgement

This work was supported by the National Science Foundation (Grant No. 10302019).

References

[1] L. Hermans, H. Vander Auweraer, Modal testing and analysis of structures under operational conditions: industrial applications, *Mechanical Systems and Signal Processing* 13 (2) (1999) 193–216.

[2] B. Cauberghe, P. Guillaume, P. Verboven, E. Parloo, Identification of modal parameters including unmeasured forces and transient effects, *Journal of Sound and Vibration* 265 (2003) 609–625.
[3] B. Peeters, G. De Roeck, Stochastic system identification for operational modal analysis: a review, *Journal of Dynamic Systems, Measurement, and Control* 123 (12) (2001) 659–667.
[4] Y. Zhang, Z. Zhang, X. Xu, H. Hua, Modal parameter identification using response data only, *Journal of Sound and Vibration* 282 (2005) 367–380.
[5] J. Lardies, State-space identification of vibrating systems from multi-output measurements, *Mechanical Systems and Signal Processing* 12 (4) (1998) 543–558.
[6] F. Tasker, A. Bosse, S. Fisher, Real-time modal parameter estimation using subspace methods: theory, *Mechanical Systems and Signal Processing* 12 (6) (1998) 686–797.
[7] N. Mastronardi, D. Kressner, V. Sima, P. Van Dooren, S. Van Huffel, A fast algorithm for subspace state-space system identification via exploitation of the displacement structure, *Journal of Computational and Applied Mathematics* 132 (2001) 71–81.
[8] C. Gontier, Energetic classifying of vibration modes in subspace stochastic modal analysis, *Mechanical Systems and Signal Processing* 19 (2005) 1–19.
[9] B. Peeters, C.E. Ventura, Comparative study of model analysis techniques for bridge dynamic characteristics, *Mechanical Systems and Signal Processing* 17 (5) (2003) 965–988.
[10] G.H. James, T.G. Carne, J.P. Lauffer, The natural excitation technique (NExT) for modal parameter extraction from operating structures, *International Journal of Analytical and Experimental Modal Analysis* 10 (4) (1995) 260–277.
[11] M. Abdelghani, M. Verhaegen, P. Van Overschee, B. De Moor, Comparison study of subspace identification methods applied to flexible structures, *Mechanical Systems and Signal Processing* 12 (5) (1998) 568–581.
[12] B. Peeters, G. De Roeck, Reference-based stochastic subspace identification for output-only modal analysis, *Mechanical Systems and Signal Processing* 13 (6) (1999) 855–878.
[13] J.B. Bodeux, J.C. Golinval, Modal identification and damage detection using the data-driven stochastic subspace and ARMAV methods, *Mechanical Systems and Signal Processing* 17 (1) (2003) 83–89.
[14] P. Van Overschee, B. De Moor, *Subspace Identification for Linear Systems: Theory, Implementation, Applications*, Kluwer Academic Publishers, Dordrecht, 1996.
[15] Y.Y. Li, L.H. Yam, Study on model order determination of thin plate systems with parameter uncertainties, *Mechanical Systems and Signal Processing* 13 (4) (1999) 667–680.
[16] D. Bauer, Order estimation for subspace methods, *Automatica* 37 (2001) 1561–1573.
[17] J. Lardies, N. Larbi, A new method for model order selection and modal parameter estimation in time domain, *Journal of Sound and Vibration* 245 (2) (2001) 187–203.
[18] G. Camba-Mendez, G. Kapetanios, Testing the rank of the Hankel covariance matrix: a statistical approach, *IEEE Transactions on Automatic Control* 46 (2) (2001) 331–336.
[19] R. Brincker, L. ingmi Zhang, et al., Modal identification of output-only systems using frequency domain decomposition, *Smart Materials and Structures* 10 (2001) 441–445.